HHS Public Access

Author manuscript

Stem Cells. Author manuscript; available in PMC 2016 June 01.

Published in final edited form as:

Stem Cells. 2015 June ; 33(6): 1743–1758. doi:10.1002/stem.1987.

Continuous Non-cell Autonomous Reprogramming to Generate Retinal Ganglion Cells for Glaucomatous Neuropathy

Sowmya Parameswaran[1], **Shashank Manohar Dravid**[2], **Pooja Teotia**[1], **Raghu R. Krishnamoorthy**[3], **Fang Qiu**[4], **Carol Toris**[1], **John Morrison**[5], and **Iqbal Ahmad**[1]

[1]Ophthalmology and Visual Sciences, University of Nebraska Medical Center, Omaha, NE

[2]Pharmacology, Creighton University, Omaha, NE

[3]Cell Biology and Anatomy, UNT Health Science Center, Fort Worth, TX

[4]Department of Biostatistics, College of Public Health, University of Nebraska Medical Center, Omaha, NE

[5]Casey Eye Institute, Oregon Health & Science University, Portland, OR

Abstract

Glaucoma, where the retinal ganglion cells (RGCs) carrying the visual signals from the retina to the visual centers in the brain are progressively lost, is the most common cause of irreversible blindness. The management approaches, whether surgical, pharmacological, or neuroprotective do not reverse the degenerative changes. The stem cell approach to replace dead RGCs is a viable option but currently faces several barriers, such as the lack of a renewable, safe, and ethical source of RGCs that are functional and could establish contacts with bona fide targets. To address these barriers, we have derived RGCs from the easily accessible adult limbal cells, re-programmed to pluripotency by a non nucleic acid approach, thus circumventing the risk of insertional mutagenesis. The generation of RGCs from the induced pluripotent stem (iPS) cells, also accomplished non-cell autonomously, recapitulated the developmental mechanism, ensuring the predictability and stability of the acquired phenotype, comparable to that of native RGCs at biochemical, molecular and functional levels. More importantly, the induced RGCs expressed axonal guidance molecules and demonstrated the potential to establish contacts with specific targets. Furthermore, when transplanted in the rat model of ocular hypertension, these cells incorporated into the host RGC layer and expressed RGC-specific markers. Transplantation of these cells in immune-deficient mice did not produce tumors. Together, our results posit retinal progenitors generated from non-nucleic acid-derived iPS cells as a safe and robust source of RGCs for replacing dead RGCs in glaucoma.

Corresponding author, Dr. Iqbal Ahmad, Professor of Ophthalmology and Visual Sciences, University of Nebraska Medical Center, 985840 Nebraska Medical Center, Omaha, NE 68198, 402-559-4091 (Office); 402-559-3238 (Fax), iahmad@unmc.edu.

Author Contributions:

Sowmya Parameswaran: Collection and assembly of data; data analysis and interpretation; manuscript writing; Shashank Manohar Dravid, Pooja Teotia, Raghu Krishnamurthy, and Fang Qiu: Collection and assembly of data; data analysis and interpretation; Carol Toris; John Morrison: Provision of study material; Iqbal Ahmad: Conception and design; data analysis and interpretation; manuscript writing.

Disclosure of Potential Conflict of Interest

The authors declare no potential conflict of interest.

Keywords

induced pluripotent stem cells; retinal ganglion cells; non-cell autonomous; glaucoma; teratoma

INTRODUCTION

Glaucoma is the most prevalent optic neuropathy where a progressive degeneration of RGCs leads to irreversible vision loss [1]. A variety of neuroprotective approaches to prolong RGC survival in animal models of glaucoma have been tested with success [2]. However, these approaches do not replace RGCs already having succumbed to the disease. Given this intractable situation, stem cell therapy has emerged as a potentially viable approach to replace dead RGCs [2–4]. However, the use of stem cells for RGC replacement is currently fraught with several barriers. Foremost, is the absence of a safe and non-immunogenic stem cell source of RGCs that can sustain practical clinical use. Second, is the lack of information about the molecular, biochemical and functional specificity of *ex-vivo* generated RGCs. Third, it is unknown if *ex-vivo* generated RGCs can elaborate guidable axons with target specificity, essential for the functional outcome of an *ex-vivo* cell therapy approach. Lastly, it is not known if the stem cell-derived RGCs possessed the potential to form teratomas. We have begun examining these barriers to *ex-vivo* stem cell approaches and addressing them through the iPS cell technology [5] under the hypothesis that iPS cells derived by non-nucleic acid approach represent a robust and safer source of RGCs for addressing degenerative changes in glaucomatous neuropathy.

Recent studies have demonstrated that the iPS cells can be a renewable source of autologous cell therapy [6], but suffers from the risk of insertional mutagenesis due to virus-mediated over-expression of reprogramming factors, Oct4, Klf4, Sox2, and cMyc (OKSM) [6]. Though this problem is being mitigated by alternate approaches of delivering the reprogramming factors, the risk of malignant transformation of the reprogrammed cells remains due to the oncogenic potential of the reprogramming factors[7]. To overcome this limitation, we have developed a non nucleic acid approach, where adult somatic progenitors from the rodent limbus, the regenerative tissue around the cornea, are reprogrammed to pluripotency under the influence of the primitive embryonic environment, simulated *in vitro* by the mouse ES cell conditioned medium. Limbal progenitors obtained from adult mouse eyes were expanded and serially reprogrammed in the presence of mouse ES cell conditioned medium, followed by the generation of retinal progenitors. The iPS cell-derived retinal progenitors were directly differentiated into RGCs in continuum by recapitulating developmental mechanisms under the influence of early retinal histogenic environment, simulated *in vitro* by conditioned medium obtained from the embryonic retinal cells. The *de novo* generated RGCs displayed biochemical and functional features of the native RGCs and demonstrated relatedness at the genomic levels with RGCs enriched from the adult mouse retina. These cells expressed receptors involved in axonal guidance of RGCs to specific targets, and demonstrated the ability to elaborate processes selectively toward mesencephalic tectal targets in an *in vitro* assay. Furthermore, retinal progenitors pre-induced along the RGC lineage, when transplanted intra-vitreally in the rat model of ocular hypertension, integrated in the host's RGC layer and expressed markers corresponding to

RGCs. They were observed elaborating apical processes toward the inner retina where the pre-synaptic neurons, bipolar cells are localized. In addition, sub cutaneous transplantation of these cells in immune-deficient mice failed to generate teratomas, demonstrating their safety. Together, these observations suggest that iPS cells, reprogrammed non-cell autonomously through a non nucleic acid niche-based approach, represent a safer and robust *ex-vivo* source of RGCs, fulfilling the initial criteria required for replacing degenerated RGCs in glaucoma.

MATERIALS AND METHODS

Animals

All experiments were conducted in accordance to the ARVO Statement for the Use of Animals in Ophthalmic and Vision Research, and were approved by the Institutional Animal Care and Use Committee (IACUC), at University of Nebraska Medical Center. Animals (mice and rats) were housed and bred in the Department of Comparative Medicine at University of Nebraska Medical Center. C57Bl6 mice were used for all experiments except the transplantation and teratoma assays. Sprague Dawley rats were used as donor cells and Brown Norway rats with ocular hypertension were used as recipients in the transplantation assays. NOD-SCID gamma (NSG) mice were used for teratoma assays.

Reprogramming and RGC generation

Limbal progenitors, enriched as neurospheres, were reprogrammed to pluripotency under the influence of mouse ES cells and neurally induced as previously described [8]. Briefly, secondary limbal neurospheres were cultured in equal volumes of embryonic stem cell conditioned medium and DMEM F12, containing N2 supplement (1×), 2 mM Glutamine, and 1% FBS (1:1) for the first 5 days. MAPK inhibitor (PD0325901;1 μM) (Stemgent) and GSK3β inhibitor (CHIR99021; 3 μM) (Stemgent) were added to the medium and culturing was continued until the appearance of ES like colonies under feeder-free conditions. For neural induction, EBs were generated by the hanging drop method in the presence of Noggin (100ng/ml), and DKK1 (100ng/ml) for 5 days. Briefly, cells were cultured in 50μl droplets (100 cells/droplet) inside a lid of Petri dish with PBS beneath for 3 days at 37°C. Cell aggregates in droplets were transferred and maintained in suspension culture in the medium containing Noggin and DKK1 for two more days to allow the formation of EBs. The EBs thus formed were subsequently cultured in neural induction medium (DMEM-F12, N2 supplement, glutamine, B27 supplement, insulin, transferrin, sodium selenite, fibronectin (ITSFn), Noggin (100 ng/ml), for 10 days at 37°C. The resulting colonies were manually triturated and cultured in neural expansion medium (neural induction medium with 20 ng/ml of fibroblast growth factor-2 (FGF2) (R&D Systems Inc., Minneapolis, MN) on poly-D-lysine (PDL) utilizing laminin-coated coverslips for 25 days to enrich RPCs. Finally, cells were plated on the PDL and laminin coated coverslips and cultured in retinal culture medium (RCM; DMEM/F12, N2 supplement, glutamine), containing equal volume of conditioned medium from E14 rat retinal cells (=E14CM) for 15 days. The chemically defined medium (=CDM) contained Shh (200ng/ml), FGF8 (100ng/ml), and DAPT (3μM) in the first two days of culture. Subsequent to that, it contained DAPT (3μM), cyclopamine (1μg/ml), and follistatin (100ng/ml).

Colliculus Aggregate culture

To determine the target specificity, the induced cells were incubated with 5 μM carboxyfluorescein diacetate (CFDA) at 37°C for ten minutes followed by washing and further incubation with culture medium at 37C for half an hour. The labeled cells were co-cultured with aggregates of cell dissociates from PN 1/PN3 superior/inferior colliculus on poly-D-lysine (PDL) and laminin-coated coverslips (n=6) for two weeks. The experiment was repeated twice.

Preparation of E14 conditioned medium

Embryonic day 14 Sprague Dawley embryos were enucleated and retinae were harvested. Retinae were dissociated using 1% Trypsin and EDTA and cultured in RCM with 1% FBS for three days. The E14 conditioned medium (E14CM) was collected after three days of culture, centrifuged to remove cells, filtered using 0.2μm filters, and stored at −80°C.

Quantitative polymerase chain reaction analysis

Quantitative polymerase chain reaction (Q-PCR) analysis was carried out as previously described [9]. Briefly, total RNA was extracted from cells using the Mini-RNeasy Kit according to the manufacturer's instructions. Complementary DNA synthesis was carried out on 5 μg of the total RNA/sample using the Superscript III RT kit following the manufacturer's instructions. Transcripts were amplified and their levels quantified using gene specific primers (Supplementary data Table S1) and Quantifast SYBR Green PCR Kit (Qiagen Inc., Valencia, CA) on Rotor Gene 6,000 (Corbett Robotics, San Francisco, CA). Measurements were performed in triplicates. A reverse-transcription-negative blank of each sample and a no-template blank served as negative controls. Amplification curves and gene expression were normalized to the housekeeping gene, GAPDH.

Immunofluorescence analysis

Immunocytochemical analysis was carried out for the detection of cell-specific markers as previously described [10]. Briefly, paraformaldehyde-fixed cells or cryostat sections were incubated in phosphate buffered saline, containing 5% normal goat serum or normal donkey serum and 0%, 0.2%, or 0.4% Triton-X100, followed by an overnight incubation in antibodies at 4°C. The list of antibodies used is given as supplementary data (Table S2). Cells were examined for epifluorescence following incubation in IgG conjugated to Cy3/FITC. Images were captured using a cooled CCD-camera (Princeton Instruments NJ, USA) and Openlab software (Improvision, MA, USA). In some cases, images were acquired using a Zeiss ApoTome Imager M2 microscope (Axiovert 200M) and captured by cooled CCD-camera (Zeiss). Axiovision 4.8 software was used for further image processing. Quantification of specific marker is presented as percentage of total DAPI positive cells. Five fields of four chambers of chamber slide or three coverslips were counted per experiment. Results were derived from three separate experiments.

Microarray Analysis

Transcriptional profiling of cells in different stages of induction was done by microarray analysis as previously described [10].Briefly, total RNA was isolated from E14 retina, iPS

cells, iPS cells derived retinal progenitors, Thy1.2$^+$ retinal RGCs, Thy1.2$^+$ iPS cell-derived RGCs and used to synthesize biotin-labeled cRNA probe, using a Gene Chip 30 IVT Express Kit (Affymetrix, Santa Clara, CA). Fragmented cRNA probes were hybridized to Genechip Mouse genome 430 2.0 arrays (Affymetrix) at 45°C for 16 hours. The arrays were scanned using an Affymetrix GCS3000 7G device, and images were analyzed using GCOS software (Affymetrix, CA, USA). Normalization and expression values were calculated using log scale robust multi-array analysis, implemented in BioConductor [11].

Thy1.2 purification of retinal RGCs and iPS cell-derived RGCs

Thy1.2 purification of the cells was carried out using magnetic bead based separation protocol. Postnatal day 2 (PN2) mice retinae (n=36–40) and/or iPSC derived RGCs (at the end of differentiation) were dissociated using Papain dissociation system (Worthington Biochemical Corporation) strictly adhering to manufacturer's protocol. The cells thus obtained were blocked with anti-mouse CD16/CD32 mab 2.4G2 (BD Biosciences) (0.25mg / 1× 10^6 cells) for 15 minutes. Cells were washed with RGC medium [serum-free modified NB-Sato medium (Neurobasal Medium (Invitrogen), bovine serum albumin (100 μg/ml), sodium selenite (40 ng/ml), putrescine (16 μg/ml), triiodo-thyronine (1.6 μg/ml), apo-transferrin (100 μg/ml), and progesterone (60 ng/ml), glutamine (2 mM), triiodo-thyronine, N-acetyl-cysteine (5 μg/ml), insulin (5 μg/ml), B27 (Invitrogen) , Ciliary neurotrophic factor (10 ng/ml), brain-derived neurotrophic factor (50 ng/ml), and forskolin (10 μM)] by centrifuging at 1000 rpm for 5 minutes. Cell pellet was treated with anti mouse CD11b magnetic particles (BD biosciences) (25mg / 1× 10^7 cells) for 30 minutes on ice to remove microglia contamination. The microglia containing magnetic particles were removed by placing the tube on imagnet. The supernatant, devoid of magnetic particles, was centrifuged at 1000rpm for 5 minutes. The cell pellets were treated with anti mouse CD90.2 (Thy1.2) magnetic particles (BD Biosciences) (25mg/1× 10^7 cells) for 30 minutes on ice to enrich for RGC cells. The magnetic particles were retrieved by placing the tube on Imagnet, and washed thrice with RGC medium to recover cells for RNA extraction. Possible contamination with thymocytes and lymphocytes, which also express Thy1 antigen, was ruled out by the absence of the detection calls for all probe sets for CD4 (thymocytes) and all except one probe sets for CD8 (lymphocytes) in the microarray results. The probe set for CD8 with the positive detection call had the low expression intensity, less than the first quartile of the intensity distributions.

Electrophysiological recordings

Whole-cell recordings were obtained from the cultured neurons at room temperature (22°C–25°C). An external solution containing (in mM) 150 NaCl, 3 KCl, 10 HEPES, 6 mannitol, 1.5 $MgCl_2$, and 2.5 CaCl2 (pH 7.4) was used for the recordings. Whole-cell patch recordings were obtained in voltage-clamp or current-clamp configuration with an Axopatch 200B (Molecular Devices, CA) and a pipette resistance of 5–8 mΩ. The internal solution for voltage-clamp recording consisted of (in mM) 150 $KMeSO_4$, 10 KCl, 0.1 EGTA, 10 HEPES, 0.3 Na_2GTP, and 0.2 Na_2ATP (pH 7.3). Loose-patch recordings were obtained using the same internal solution. No channel blockers or inhibitors were used during loose-patch recording. Recordings were corrected for junction potential. Signal was filtered at 2

kHz and digitized at 10 kHz using an Axon Digidata 1440A analog-to-digital board (Molecular Devices, CA).

Induction of ocular hypertension

The surgical procedure of Morrison et al., 1997 [12]was used to elevate the intraocular pressure in Brown Norway rats. In brief, retired breeders weighing between 200–300g, with stabilized and reliable IOP measurements were maintained in reduced constant light environment of 90 lux for a minimum of three days prior to surgery. After three days, animals were anaesthetized with intraperitoneal injection of 100μl of cocktail containing ketamine(50mg/ml), xylazine (5mg/ml) and acepromazine (1mg/ml) for every gram of body weight. One eye of each animal was injected with 1.8M hypertonic saline via an episcleral vein using a polypropylene ring fitted around the equator of the globe to occlude all other aqueous veins. Fifty microlitres of hypertonic saline were injected into the vein using a microglass needle to blanch the aqueous plexus, scarring the trabecular meshwork and elevating IOP with subsequent damage to optic nerve. The contralateral eyes served as controls. After the procedure, rats were maintained in constant low illumination of 70 lux to minimize the diurnal and nocturnal effects on IOP. Eye pressures were monitored weekly on conscious animals using Tonolab tonometer in the presence of topical anesthesia, proparacaine HCl [13].

Transplantation in rat model of ocular hypertension

Intra-vitreal transplantation of iPS cell-derived RPCs, pre-committed along the RGC lineage by culturing in E14CM for 5 days, was carried out as previously described [14]. Briefly, papain digestion was used to obtain single cells followed by labeling with 5μM CFDA (Molecular probes) as described above. CFDA labeled cells (1×10^5) were injected in 2 μl volume into the vitreous cavity of Brown Norway rats (one with ocular hypertension and the other served as a control), using glass micropipette connected to a 10μl Hamilton syringe. Unlike previously described method [14] no mechanical damage was done to the retina. Eyes were enucleated after 2–4 weeks for immunohistochemical analysis. Two individual experiments were conducted. In each experiment four animals were included for analysis.

Teratoma formation

Two million iPS cell-derived RGCs or embryonic stem cells (positive control) were injected subcutaneously into the dorsal flank of non-obese diabetic-severe combined immunodeficiency NOD-SCID gamma chain knockout (NSG) mice. Two mice per group were used for the analysis. The formation of teratoma was monitored weekly till evident. The mice were euthanized at the end of two months post-injection.

Statistical Analysis

Statistical analysis was performed using one-way analysis of variance (ANOVA) for multiple group comparisons (GraphPad Prism Software). p values less than 0.05 were considered significant. Results were obtained from three replicate samples from two individual experiments.

RESULTS

Generation of iPS cells and retinal progenitors

The adult mouse limbal progenitors were reprogrammed non-cell autonomously to pluripotency by culturing them in the presence of ES cell conditioned medium (CM), as previously described [8, 10] (Figure 1A). To increase the efficiency of reprogramming, ESCM was supplemented with MAPK and GSK3β inhibitors [10]. The reprogrammed colonies emerged by day 20 in culture, and expressed pluripotency markers, Oct4 (Figure 1B), Nanog (Figure 1C), and SSEA1 (Figure 1D). Cells in the emerging colonies maintain normal karyotype [8]. To derive retinal progenitors, the iPS cells were first differentiated along the three germ layers through the formation of embryoid bodies (EBs) in the presence of Noggin and DKK to reduce BMP and Wnt signaling, respectively. The EBs expressed markers corresponding to three primitive germ layers, Otx2 (ectoderm) (Figure 1E), Brachyury (mesoderm) (Figure 1F) and Sox 17 (Endoderm) (Figure 1G). Next, a batch of EBs was cultured in neuronal induction medium containing Noggin to reduce the neural inhibitory BMP signaling [15] for 10 days for directly differentiating them along the neuroectodermal lineage. At the end of the neural induction phase, cells expressed immunoreactivities corresponding to neuroectodermal progenitor markers, Nestin (Figure 1H) and Musashi (Figure 1I), and pro-neural transcription factor, Mash1 (Figure 1J). To demonstrate that the neural induction was not stochastic, we examined the expression of select genes at varying time intervals of neuronal induction (Figure 1K). A temporal decrease in the expression of the pluripotency gene, *Oct4*, was observed. Transcripts corresponding to cells of non-neural lineages, i.e., embryonic endodermal (*Sox17*) and mesodermal (*Brachyury*) cells that were expressed in the EBs were undetectable by day 2 of neural induction. In contrast, the expression of an early marker of the developing rostral forebrain, *Otx2* [16], increased significantly at day 2, followed by the induction of *Nestin* and *Mash1* expression, which peaked at day 8. A decrease in *Otx2* transcript levels was observed following day 2, presumably representing the silencing of *Otx2*, once neural induction was initiated. The temporal decrease in the expression of the pluripotency and non-neural genes and the reciprocal induction of the neural genes suggested a selective induction of the iPS cells along the neural lineage. To derive and expand retinal progenitors from the neurally induced iPS cells, the latter were cultured for the next 25 days in the presence of FGF2 and Noggin (Figure 2A). Given the fact that the efficiency of *de novo* RGC generation depends upon the fidelity of the generation of the retinal progenitors, the induction of iPS cells along the retinal lineage was examined by complimentary approaches. We began by comparing the transcription profiles of the induced and un-induced iPS cells to determine whether or not the induction of the iPS cells along the retinal lineage was reflected in patterns of the global gene expression. A relative divergence (R^2=0.81) in global gene expression between the two cell populations was observed, along with a remarkable up-regulation of the eye field genes, *Pax6, Rx, Six3, Chx10, Lhx2*, and *Six6* in the iPS cells after 25 days of retinal induction (Figure 2B). These genes encode transcription factors that constitute the molecular phenotype of the early retinal progenitors [17]. The acquisition of the eye field gene expression by induced cells was independently corroborated by RT-PCR (Supplementary material Figure S1); while the un-induced cells were characterized by the presence and absence of transcripts corresponding to *Oct4* and the eye field genes,

respectively, the induced cells had lost *Oct4* expression and acquired those corresponding to *Pax6, Rx, Six3, Chx10, Lhx2,* and *Six 6*. More importantly, when we compared the transcriptional profiles of the iPS cells induced along the retinal lineage with that of cells isolated from the embryonic day 14 (E14) mouse retina, which is enriched in retinal progenitors, the patterns of the global gene expression was comparable (R^2=0.90) to shared expression of the eye field genes (Figure 2C). The residual divergence can be owed to the fact that the induced cell population represented a mix of induced cells and un-induced cells in different stages of induction. Lastly, to further characterize the retinal features of induced cells, we carried out immunocytochemical analyses, which revealed a subset of cells expressing immunoreactivities corresponding to Pax6, Rx, and Chx10, (Figure 2 G–I), similar to those in E14 mouse retina (Figure 2D–F). The proportions of induced cells expressing Pax6, Rx and Chx10 were 78.43 ± 4.32%, 26.71± 2.33%, and 42.64 ± 5.30%, respectively (Figure 2J). Double immunocytochemical analysis revealed that 19.96± 2.28% (Figure 2G (inset), J) of induced iPS cells co-expressed Pax6 and Rx. The comparative transcription profiles and immunocytochemical analysis suggested that the global gene expression of iPS cells was altered under defined culture conditions, enabling a subset of them to acquire retinal progenitor properties.

Generation of RGCs

Next, we examined whether or not retinal progenitors derived from the iPS cells can differentiate into RGCs, the first cell type generated in the developing retina [18]. We cultured the iPS cell-derived retinal progenitors in conditioned medium obtained from E14 rat retinal cells (=E14CM) for 15 days (Figure 3A). The E13/14 stage represent the peak of RGC generation in rodent retina and cells at this stage elaborate evolutionarily conserved RGC promoting activities that significantly facilitate differentiation of progenitors, retinal or heterologous, along RGC lineage, compared to controls [19,20]and those differentiated in chemically defined medium (see below). First, we examined the biochemical properties of differentiated cells. A subset of cells at the end of 15 days in culture expressed immunoreactivities corresponding to the regulators of RGC differentiation, Atoh7 (43.1±1.9%), Brn3b (13.3±1.5%), and Islet1 (45.6±1.3%) (Figure 3F, G, H, J) similar to those in the E14 mouse retina (Figure 3B, C, D). A smaller subset of cells expressed mature RGC marker Thy1 (5.4±1.1%) (Figure 3I, J), as observed in the PN1 retina (Figure 3E). Since Thy1 is also expressed in extra-ocular cells, we carried out double immunocytochemistry to co-localize Thy1 and Brn3b immunoreactivities, thus confirming the RGC identity of $Thy1^+$ cells (Figure 3I; inset). Second, to determine that RGCs shared properties with the native RGCs at the genomic level, we compared the transcriptional profiles of immune-panned iPS cell-derived $Thy1.2^+$ RGCs with that of $Thy1.2^+$ RGCs immune-panned from the adult mouse retina. The Pearson correlation coefficient demonstrated a relative divergence in the global gene expression patterns (R^2=0.82) between the two cell populations (Figure 3K). However, a strong correspondence in the expression of a group of genes involved in RGC differentiation (*Atoh7, Brn3b, Pax6, Wt1, RPF1, Irx2, Brm,* and *Hes1*) and maturation (*Sncg, Thy1, Shh,* and *GAP43*), including those facilitating axonal guidance (*NRP1, DCC, EphA4, EphA3,* and *Robo2*), was observed. These RGC genes were expressed in both populations and remained within a two-fold difference. The expression of these genes was independently corroborated by RT-PCR (Supplementary

material Figure S2). The transcriptional profile also revealed that the induced RGCs expressed REST, which may influence their efficiency since it is a negative regulator of RGC differentiation [21]. While these results suggested that iPS cell-derived retinal progenitors acquired the RGC phenotype, information as to whether or not they did so by the recruitment of normal developmental mechanisms was essential to confirm the stability of the directed differentiation. Therefore, we examined the temporal expression patterns of genes that have emerged as hierarchical regulators of RGC specification/differentiation (Figure 4A) [22] during the differentiation of iPS cell-derived retinal progenitors along the RGC sub lineage (Figure 4B). A temporal decrease in the expression of *Rx* and *Chx10* was observed, as expected of markers of retinal progenitors, which are undergoing differentiation. In contrast, cells in culture acquired the expression of *Atoh7*, expected of cells being specified along the RGC lineage. The acquisition of *Atoh7* expression was followed by a temporal increase in the expression of the regulators of RGC differentiation, *Brn3b* and *Isl1*, and *RPF1* and mature RGC markers, *Sncg*, *Shh*, *Thy1*, and *GAP43*. Together, the temporal expression patterns of RGC regulators suggested that the RGC phenotype was acquired by recapitulating developmental mechanisms, predicting its stability.

Functional attributes and target selectivity of iPS cell-derived RGCs

To determine whether or not the differentiated cells possessed the functional attributes of RGCs, we first examined the current profiles by whole cell patch recordings, which might be indicative of their functional differentiation [23,24]. Cells displaying neuronal morphology (Figure 5A) were selected for electrophysiological recording. When cells were clamped at the holding potential of −90mV and currents were evoked by a series of voltage steps (−100mV to +20mV), 85.7% of them (N=14) revealed the presence of fast inward and delayed but sustained outward currents, the former being sensitive to the presence of TTX (Figure 5B). When these cells were examined in loose-patch conditions, 71.4% of them (N=15) elicited spiking activities with frequencies ranging from 0.08 to 0.3 Hz (Figure 5C). Examination of fast inward and outward currents in whole cell patch recordings showed I-V relationship typical of voltage–gated sodium and delayed potassium currents, respectively, similar to that observed in isolated RGCs from the rat [23] and primate [24] retina (Figure 5D).

Next, we tested whether the iPS cells-derived RGCs possessed attributes required for use in cell therapy of glaucomatous RGC degeneration. To determine if they demonstrated target specificity needed for functional recovery, we examined the expression of molecules that guide the RGC axons to specific targets. RT-PCR analysis of iPS cells-derived RGCs revealed that they expressed transcripts corresponding to (1) ROBO2, required for intra-retinal guidance and navigation at the optic chiasm (2), DCC, required for the exit at the optic disc (3), NEUROPILIN 1 (NRP1), required for keeping the axons coalesced (4), GAP43, essential for guiding axons from the optic chiasm into the optic tracts, and (5) EPHs which determines the spatial gradient of connections in the superior colliculus [25] (Figure 5E). Immunocytochemical analysis of select guidance molecules revealed the expression of immunoreactivities corresponding to ROBO2 and GAP43 in Brn $3b^+$ iPS cells-derived RGCs (Figure 5, F–I), corroborating the PCR results at the cellular levels. Together, these

observations suggested that the iPS cells-derived RGCs had the molecular make-up necessary to respond to guidance cues for target selection. To test the premise that these cells possess the target specificity of native RGCs, we cultured CFDA-labeled iPS cells-derived RGCs across cell aggregates from either the superior colliculus (SC) or inferior colliculus (IC). We observed that the CFDA-labeled cells, similar to RGC-derived from the late retinal progenitors [26], elaborated long processes in the presence of SC explants and oriented them toward the SC cells, the specific target of RGC axons in the mid brain (Figure 5J). The esterified fluorchrome complexes of CFDA remain trapped within the cell body, thus highlighting it, and do not stain the newly elaborated processes. The CFDA stained cells, when cultured in the presence of the IC cells, a target of the auditory neurons, elaborated short processes that failed to orient themselves toward the cell aggregates (Figure 5K). Next, to address the outstanding question of the relative efficiency of E14CM- and chemically defined medium (CDM)-mediated RGC differentiation, we carried out a side-by-side comparison of the two methods. It has been demonstrated that the CDM consisting of DAPT to reduce Notch signaling promotes RGC differentiation in mouse and human iPS cells [36, 37]. To enhance the efficiency of CDM-based method we initially exposed iPS cell-derived retinal progenitors to sonic hedgehog (Shh), fibroblast growth factor 8 (FGF8) and DAPT for two days to recapitulate engagement of signaling pathways during normal RGC differentiation [27–29]. Culture was continued thereafter in the presence of DAPT and cyclopamine, the latter to inhibit Shh signaling, which after initial induction is inhibitory to RGC differentiation [30]. Follistatin was added to inhibit TGFβ signaling, which suppresses RGC differentiation [31] (Figure 6A). Analysis of cells at the end of the differentiation protocol revealed that the levels of transcripts corresponding to Brn3b, Islet1, and Thy1 were significantly lower in CDM than in E14CM (Figure 6, B–D). To compare the extent of functional differentiation in different conditions, we first examined the current profiles of cells by whole cell patch recordings. When cells from CDM were recorded only 40% of cells revealed detectable currents (n=10). Moreover, only delayed and sustained outward currents were observed in these cells and no fast inward currents, corresponding to voltage-gated channels, were seen (Figure 6, E, F). In contrast, cells maintained in E14CM displayed the typical fast inward and sustained outward currents (n=4), seen in isolated RGCs [23, 24]. In addition, when cells were recorded in loose-patch condition, spiking activities were observed only in those cultured in E14CM (n=4) and not in CDM (n=4) (Figure 6G). Together, these results suggested that E14CM represented a more conducive condition than the given CDM for the directed differentiation of iPS-derived retinal progenitors along the RGC lineage.

Incorporation of iPS cell-derived RGCs in the ocular hypertensive rat retina

Next, we examined whether or not the nascent iPS cells-derived RGCs could incorporate in the host retina. We used Morrison's rat model of ocular hypertension [12], where blocking one of the scleral veins by injecting saline solution leads to a progressive increase in the intra-ocular pressure (IOP) due to the sclerosed trabecular (Figure 7A). The increase in IOP was followed by RGC degeneration, reflecting the glaucomatous disease conditions in humans [32]; the inner plexiform layer was thinner likely due to the loss of nerve fiber layer and areas of the ganglion cell layer lacked cells, compared to controls (Figure 7B). The degeneration in the RGC layer was not uniform. The iPS cell-derived retinal progenitors,

pre-exposed to RGC differentiation conditions, were labeled with fluorescent dye, CFDA and transplanted intravitreally in the ocular hypertensive rats. Since injuries, genetic, chemical or mechanical, facilitate the incorporation of transplanted cells in the host retina [14, 33], we expected that the pressure-related RGC degeneration would offer a similar conducive environment for transplant integration. Examination of the retinal sections two weeks after transplantation revealed a small subset of CFDA-positive cells incorporated in the host retina, predominantly in the RGC layer. The majority (~90%) of the CFDA labeled cells were observed trapped in the vitreous and a small subset of cells were observed incorporated in the host retina. Immunohistochemical analysis of the retinal sections revealed, CFDA-positive cells expressing Brn3b, suggesting the differentiation of the incorporated cells along the RGC lineage (Figure 7C). The intensity of the Brn3b staining was increased, leading to difference in cell size as compared to CFDA staining, to highlight a CFDA negative native RGC (Figure 7C, asterisk). Since Brn3b is a transcriptional factor, preferentially localized in the nuclei, its expression did not shed light on the morphology of the incorporated cells. Examination of immunoreactivities corresponding to neuronal microtubule component, β-III tubulin, which within the retina is predominantly expressed in RGCs [34] and expressed by iPS-derived RGCs (Figure 5A), revealed apical processes in the $CFDA^+$ cells, which were elaborated toward the inner nuclear layer, where RGCs receive input from bipolar cells. The cell contained short distal processes in the RGC layer (Figure 7D). Lastly, we examined the risk of teratoma formation of the transplanted cells. Screening for the teratomas one month after transplantation was negative. For a more robust test of teratoma formation, a batch of cells for retinal transplantation was injected sub-cutaneously in the immune-deficient mice. ES cells were injected as controls. Teratomas, with differentiated three germ layers, promptly developed in controls at the end of the second week post injection (Figure 7E). No teratomas were formed in mice injected with iPS cell-derived RGCs after two months, when the animals were euthanized (Figure 7E). Together, these observations suggested that the iPS cell-derived RGCs are safe, easily incorporated in the host's RGC layer, and have the ability of target discrimination, similar to native RGCs.

Discussion

Recent studies have demonstrated that the iPS cells can be a renewable source of progenitors for *ex-vivo* stem cell approaches to treat degenerative diseases including those that cause blindness [6,35]. For example, cells that are responsible for vision in low light, the rod photoreceptors, as well as RGCs can be directly differentiated from the mouse and human iPS cells [9, 36–38]. Cells in retinal pigment epithelium (RPE) that provide both mechanical and functional support to photoreceptors have been reproducibly generated from both mouse and human iPS cells [36,39]. However, in all these cases, the iPS cells were reprogrammed by the nucleic acid approach of over-expressing exogenous transcription factors, thereby conferring the risk of insertional mutagenesis. Here, we have demonstrated that RGCs can be reproducibly derived from the iPS cells, which may be relatively safe from the risk of insertional mutagenesis and teratoma formation. To address the safety issues of insertional mutagenesis, we reprogrammed limbal cells to pluripotency followed by their induction along the RGC lineage non-cell autonomously, based on the emerging information that stem

cells and their progenies are profoundly influenced by their microenvironments. For example, during development, as well as in the adults, the regulation of stem cells by their niches not only assists them in maintaining a quiescent state but also facilitates temporal reprogramming thus allowing them to generate specific cell types [40–43]. Consequently, when niches are experimentally altered the status and potential of stem cells are affected such that older progenitors are rejuvenated when placed in a younger niche [19, 44], thereby suggesting that niche-dependent reprogramming to a relatively primitive stage is a possibility. These observations, including the seminal one by Martin (1981)[45] that embryonal carcinoma cell CM could help generate and maintain ES cells suggest that here, the ESCM provided the primitive environment for retrograde reprogramming of the somatic progenitors. Apart from the observation that both protein- and nucleic acid (exosomal miRNA)-based activities in the ESCM influenced the retrograde reprogramming [10], the underlying mechanism of how these activities interact with the cell-intrinsic factors for pluripotency remains to be elucidated. However, two intrinsic properties of limbal progenitors may play important roles in making these progenitors responsive to ESCM reprogramming activities. First, the limbal progenitors express three (i.e., KSM) of the four reprogramming factors, which may leave the genome of these cells poised for pluripotency. Second, unlike fibroblasts limbal progenitors are epithelial in nature, which may eliminate the requirement of the mesenchymal to epithelial transition (MET) steps from reprogramming.

For the directed differentiation of the iPS cell-derived retinal progenitors into RGCs we used a non cell-autonomous approach that utilizes the dynamic retinal niche during development, where seven different cell types are generated in an evolutionarily conserved and temporally segregated stages of early and late histogenesis [46]. Notably, RGCs are the first cells born across species [47]. Evidence suggests that the early histogenic niche, between E13.5-E14 in the rodent retina when the majority of RGCs are generated, is enriched in RGC promoting activities [19]. These activities are elaborated by E14 retinal cells in culture medium, thus directing the differentiation of retinal or non-retinal neural progenitors into RGCs, compared to FBS controls [19, 20]. Differentiation of the iPS cell-derived retinal progenitors along the RGC lineage under the influence of a simulated early histogenic environment provided by E14CM has advantages over other approaches [37, 38]. First, this approach tests the inherent capacity of the iPS cell-derived retinal progenitors to respond to RGC-specific histogenic cues. Second, it facilitates the developmental mechanism in the responding cells essential for the efficient acquisition of the RGC phenotype, without the ectopic expression of exogenous *Atoh7* [38], thus mitigating the risk of insertional mutagenesis. Previous studies on directed differentiation of iPS cells into RGCs under the influence of reduced Notch signaling [37] or through the combination of reduced Notch signaling and ectopic expression of Atoh7 [38] largely examined the RGC phenotype finally acquired and not the mechanism(s) by which it was acquired. Here, we demonstrate that under the influence of E14CM, the iPS cell-derived retinal progenitors mobilize a normal mechanism of RGC differentiation. For example, initially these cells are characterized by the presence of transcripts corresponding to *Pax6*, *Rx*, and *Hes1* demonstrating their undifferentiated status, presumably under active Notch signaling (indicated by *Hes1* expression), which is inhibitory to proneural genes, such as *Atoh7* [48]. However, when these cells are cultured in E14CM,

Atoh7 gene is activated accompanied by decreased expression of *Hes1* (data not shown), recapitulating the role of Notch signaling during the specification of RGCs [49]. Besides, Atoh7, several transcription factors regulate RGC differentiation. The temporal emergence of the expression of transcripts corresponding to *Brn3b*, *Isl1*, and *RPF1*, following the activation of *Atoh7*, suggests that these genes are activated downstream of *Atoh7* [22]. Additionally, the differentiating cells express transcripts that encode chromatin-remodeling enzyme, Brm, and Zinc finger transcription factor, Wt1, which play important role in the activation of *Brn3b* and *Shh* expression [50]. Taken together, these observations suggest the likely recapitulation of the hierarchical regulatory mechanism for RGC differentiation by the iPS cell-derived neural progenitors under E14CM, thus predicting stability of the acquired phenotype. The side-by-side comparison of RGC differentiation under the influence of either E14CM or CDM, where CDM contained factors and small molecules to engage signaling pathways involved in RGC differentiation *in vivo*, suggests that E14CM may offer a relatively conducive environment compared to CDM for differentiation in terms of efficiency and functional maturation. However, this conclusion is with a caveat that with the examination of the dose of these factors/small molecules and timing of their presentation to the responding cells the efficiency of CDM-mediated directed differentiation can be improved.

It is important to note that based on the relative expression of RGC-specific regulators and mature markers, it could be inferred that not all iPS cell-derived neural progenitors that are specified along the RGC lineage fully recapitulate the regulatory hierarchy. For example, the proportions of cells with immunoreactivities corresponding to Atoh7, Brn3b, and Thy1 at the end of RGC differentiation were 43%, 13%, and 5%, respectively. These proportions suggest that only a small subset of specified cells attain the maturity, defined by the expression of Brn3b/Thy1. This observation carries important implications. In particular, it suggests that the prediction of the efficiency of RGC differentiation is as good as the markers used. For example, the use of more primitive and permissive markers, such as Isl1, can likely overestimate the efficiency of RGC differentiation. On the other hand, the use of more mature RGC markers, such as Brn3b or Thy1, to identify transplanted cells may underestimate cells that are along a bonafide RGC lineage but have not matured enough to express Brn3b/Thy1, thus underestimating the number of potential RGCs incorporated in the host retina (see below). The inability of a subset of cells to fully recapitulate the regulatory hierarchy might be due to inadequate differentiation conditions (time and factors) or inhibitory factors intrinsic to the iPS cells or both. For example, the relatively higher expression of REST in the iPS cell-derived RGCs, compared to the native RGCs, may attenuate the transition of specified cells along the regulatory hierarchy, affecting their maturity and thus contributing to the divergence in the global gene expression patterns between the two populations (Figure 3K). This notion is supported by the observation that the loss of function of REST in ES-cell derived retinal progenitors significantly increased the expression of RGC regulators and mature markers, compared to controls (data not shown). Taken together, the selective gene expression suggests that a subset of iPS cell-derived retinal progenitors, albeit small, recapitulate the normal RGC developmental mechanism, which may predict the stability of their phenotype, essential for functionally replacing degenerated RGCs.

Furthermore, our observations suggest that iPS cell-derived RGCs fulfill the following two basic criteria required to support cell therapy for glaucomatous RGC degeneration: 1) the capacity to differentiate into RGCs *in vivo* and 2), elaborate processes, capable of path finding and reaching their targets. The second criterion was analyzed only *in vitro*. To the best of our knowledge these criteria remained un-investigated in iPS cells. First, the iPS cell-derived retinal progenitors, when transplanted intravitreally in rats with ocular hypertension, incorporated into the host retina. Such incorporation was not observed in controls, which supports previous observations that lamina-specific incorporation requires the degeneration of specific retinal neurons [14]. Importantly, the incorporated cells expressed Brn3b, which suggests their differentiation into RGCs *in vivo*. Although it remains to be demonstrated whether the transplanted RGCs can integrate synaptically within the inner retina the apically oriented βtubulin^{+} process of a transplanted cell suggests such a possibility. Second, the iPS cell-derived RGCs expressed several of axonal guidance molecules, which suggests their potential to functionally replace degenerated RGCs. RGC axons face decision points at several locations in the visual pathway, and their guidance depends on the ability of their growth cones to sense the environment at each of these locations [25]. Therefore, the axons of iPS cell-derived RGCs may be able to navigate the environment to reach the targets. Although this too remains to be demonstrated, our observations that the iPS cell-derived RGCs elaborate processes toward SC cells, which are the bonafide RGC target and not IC cells, is a preliminary indication of the ability of these cells' functional competence. Additionally, unlike RGCs derived from nucleic acid-generated iPS cells under the influence of reduced Notch signaling and ectopic expression of *Atoh7* [38], RGCs generated from the non-cell autonomous iPS cells under the influence of E14CM did not form teratomas, one month post-intravitreal transplantation or when transplanted sub-cutaneously in immune deficient mice, thus demonstrating the relative safety of the approach.

CONCLUSION

Together, our observations posit the non-cell autonomously derived iPS cells as a relatively robust and safe source of retinal progenitors for generating RGCs with target specificity, allowing their potential use in replacing degenerated RGCs in glaucomatous neuropathy.

Supplementary Material

Refer to Web version on PubMed Central for supplementary material.

ACKNOWLEDGEMENTS

The research was supported by NIH (NEI; R01-EY022051). Thanks are due to Qulsum Mir, Sharada Paudel, and John Sorrentino for technical help, Li Zheng for schematics, and Dr. Graham Sharp for critical reading of the manuscript.

References

1. Coleman AL. Glaucoma. Lancet. 1999; 354:1803–1810.
2. Dahlmann-Noor AH, Vijay S, Limb GA, et al. Strategies for optic nerve rescue and regeneration in glaucoma and other optic neuropathies. Drug Discov Today. 2010; 15:287–299. [PubMed: 20197108]

3. Johnson TV, Martin KR. Cell transplantation approaches to retinal ganglion cell neuroprotection in glaucoma. Curr Opin Pharmacol. 2013; 13:78–82. [PubMed: 22939899]
4. Levin LA, Ritch R, Richards JE, et al. Stem cell therapy for ocular disorders. Arch Ophthalmol. 2004; 122:621–627. [PubMed: 15078681]
5. Parameswaran S, Balasubramanian S, Rao MS, et al. Concise review: non-cell autonomous reprogramming: a nucleic acid-free approach to induction of pluripotency. Stem Cells. 2011; 29:1013–1020.
6. Takahashi K, Yamanaka S. Induced pluripotent stem cells in medicine and biology. Development. 2013; 140:2457–2461. [PubMed: 23715538]
7. Barrilleaux B, Knoepfler PS. Inducing iPSCs to escape the dish. Cell Stem Cell. 2011; 9:103–111. [PubMed: 21816362]
8. Balasubramanian S, Babai N, Chaudhuri A, et al. Non cell-autonomous reprogramming of adult ocular progenitors: generation of pluripotent stem cells without exogenous transcription factors. Stem Cells. 2009; 27:3053–3062. [PubMed: 19859985]
9. Parameswaran S, Balasubramanian S, Babai N, et al. Induced pluripotent stem cells generate both retinal ganglion cells and photoreceptors: therapeutic implications in degenerative changes in glaucoma and age-related macular degeneration. Stem Cells. 2010; 28:695–703. [PubMed: 20166150]
10. Parameswaran S, Balasubramanian S, Babai N, et al. Nucleic acid and non-nucleic acid-based reprogramming of adult limbal progenitors to pluripotency. PLoS One. 2012; 7:e46734. [PubMed: 23056428]
11. Bolstad, BMIR.; Gautier, L.; Wu, Z. Preprocessing High-density Oligonucleotide Arrays in Bioinformatics and Computational Biology Solutions Using R and Bioconductor. Springer; 2005. (2005), Springer, 2005.
12. Morrison JC, Moore CG, Deppmeier LM, et al. A rat model of chronic pressure-induced optic nerve damage. Exp Eye Res. 1997; 64:85–96. [PubMed: 9093024]
13. He S, Minton AZ, Ma HY, et al. Involvement of AP-1 and C/EBPbeta in upregulation of endothelin B (ETB) receptor expression in a rodent model of glaucoma. PLoS One. 2013; 8:e79183. [PubMed: 24265756]
14. Chacko DM, Das AV, Zhao X, et al. Transplantation of ocular stem cells: the role of injury in incorporation and differentiation of grafted cells in the retina. Vision Res. 2003; 43:937–946. [PubMed: 12668063]
15. McMahon JA, Takada S, Zimmerman LB, et al. Noggin-mediated antagonism of BMP signaling is required for growth and patterning of the neural tube and somite. Genes Dev. 1998; 12:1438–1452. [PubMed: 9585504]
16. Puelles E, Acampora D, Lacroix E, et al. Otx dose-dependent integrated control of antero-posterior and dorso-ventral patterning of midbrain. Nat Neurosci. 2003; 6:453–460. [PubMed: 12652306]
17. Zuber ME, Gestri G, Viczian AS, et al. Specification of the vertebrate eye by a network of eye field transcription factors. Development. 2003; 130:5155–5167. [PubMed: 12944429]
18. Agathocleous M, Harris WA. From progenitors to differentiated cells in the vertebrate retina. Annu Rev Cell Dev Biol. 2009; 25:45–69. [PubMed: 19575661]
19. James J, Das AV, Bhattacharya S, et al. In vitro generation of early-born neurons from late retinal progenitors. J Neurosci. 2003; 23:8193–8203. [PubMed: 12967980]
20. Del Debbio CB, Peng X, Xiong H, et al. Adult ciliary epithelial stem cells generate functional neurons and differentiate into both early and late born retinal neurons under non-cell autonomous influences. BMC Neurosci. 2013; 14:130. [PubMed: 24148749]
21. Mao CA, Tsai WW, Cho JH, et al. Neuronal transcriptional repressor REST suppresses an Atoh7-independent program for initiating retinal ganglion cell development. Dev Biol. 2011; 349:90–99. [PubMed: 20969844]
22. Mu X, Fu X, Sun H, et al. A gene network downstream of transcription factor Math5 regulates retinal progenitor cell competence and ganglion cell fate. Dev Biol. 2005; 280:467–481. [PubMed: 15882586]
23. Lipton SA, Tauck DL. Voltage-dependent conductances of solitary ganglion cells dissociated from the rat retina. J Physiol. 1987; 385:361–391. [PubMed: 2443669]

24. Han Y, Jacoby RA, Wu SM. Morphological and electrophysiological properties of dissociated primate retinal cells. Brain Res. 2000; 875:175–186. [PubMed: 10967314]
25. Erskine L, Herrera E. The retinal ganglion cell axon's journey: insights into molecular mechanisms of axon guidance. Dev Biol. 2007; 308:1–14. [PubMed: 17560562]
26. Das, AV.; James, J.; Edakkot, S., et al. Retinal Stem Cells. In: R, M., editor. Neural Development and Stem Cells. Totowa, NJ: Humana Press Inc.; 2005. p. 235-247.
27. Martinez-Morales JR, Del Bene F, Nica G, et al. Differentiation of the vertebrate retina is coordinated by an FGF signaling center. Dev Cell. 2005; 8:565–574. [PubMed: 15809038]
28. Ahmad I, Dooley CM, Polk DL. Delta-1 is a regulator of neurogenesis in the vertebrate retina. Dev Biol. 1997; 185:92–103. [PubMed: 9169053]
29. Neumann CJ, Nuesslein-Volhard C. Patterning of the zebrafish retina by a wave of sonic hedgehog activity. Science. 2000; 289:2137–2139. [PubMed: 11000118]
30. Wang Y, Dakubo GD, Thurig S, et al. Retinal ganglion cell-derived sonic hedgehog locally controls proliferation and the timing of RGC development in the embryonic mouse retina. Development. 2005; 132:5103–5113. [PubMed: 16236765]
31. Kim J, Wu HH, Lander AD, et al. GDF11 controls the timing of progenitor cell competence in developing retina. Science. 2005; 308:1927–1930. [PubMed: 15976303]
32. Minton AZ, Phatak NR, Stankowska DL, et al. Endothelin B receptors contribute to retinal ganglion cell loss in a rat model of glaucoma. PLoS One. 2012; 7:e43199. [PubMed: 22916224]
33. Pearson RA, Barber AC, West EL, et al. Targeted disruption of outer limiting membrane junctional proteins (Crb1 and ZO-1) increases integration of transplanted photoreceptor precursors into the adult wild-type and degenerating retina. Cell Transplant. 2010; 19:487–503. [PubMed: 20089206]
34. Sharma RK, Netland PA. Early born lineage of retinal neurons express class III beta-tubulin isotype. Brain Res. 2007; 1176:11–17. [PubMed: 17900541]
35. Cramer AO, MacLaren RE. Translating induced pluripotent stem cells from bench to bedside: application to retinal diseases. Curr Gene Ther. 2013; 13:139–151. [PubMed: 23320477]
36. Hirami Y, Osakada F, Takahashi K, et al. Generation of retinal cells from mouse and human induced pluripotent stem cells. Neurosci Lett. 2009; 458:126–131. [PubMed: 19379795]
37. Riazifar H, Jia Y, Chen J, et al. Chemically induced specification of retinal ganglion cells from human embryonic and induced pluripotent stem cells. Stem Cells Transl Med. 2014; 3:424–432. [PubMed: 24493857]
38. Chen M, Chen Q, Sun X, et al. Generation of retinal ganglion-like cells from reprogrammed mouse fibroblasts. Invest Ophthalmol Vis Sci. 2010; 51:5970–5978. [PubMed: 20484577]
39. Buchholz DE, Pennington BO, Croze RH, et al. Rapid and efficient directed differentiation of human pluripotent stem cells into retinal pigmented epithelium. Stem Cells Transl Med. 2013; 2:384–393. [PubMed: 23599499]
40. Calvi LM, Adams GB, Weibrecht KW, et al. Osteoblastic cells regulate the haematopoietic stem cell niche. Nature. 2003; 425:841–846. [PubMed: 14574413]
41. Yeung TM, Chia LA, Kosinski CM, et al. Regulation of self-renewal and differentiation by the intestinal stem cell niche. Cell Mol Life Sci. 2011; 68:2513–2523. [PubMed: 21509540]
42. Kuang S, Gillespie MA, Rudnicki MA. Niche regulation of muscle satellite cell self-renewal and differentiation. Cell Stem Cell. 2008; 2:22–31. [PubMed: 18371418]
43. Riquelme PA, Drapeau E, Doetsch F. Brain micro-ecologies: neural stem cell niches in the adult mammalian brain. Philos Trans R Soc Lond B Biol Sci. 2008; 363:123–137. [PubMed: 17322003]
44. Conboy IM, Conboy MJ, Wagers AJ, et al. Rejuvenation of aged progenitor cells by exposure to a young systemic environment. Nature. 2005; 433:760–764. [PubMed: 15716955]
45. Martin GR. Isolation of a pluripotent cell line from early mouse embryos cultured in medium conditioned by teratocarcinoma stem cells. Proc Natl Acad Sci U S A. 1981; 78:7634–7638. [PubMed: 6950406]
46. Rapaport DH, Wong LL, Wood ED, et al. Timing and topography of cell genesis in the rat retina. J Comp Neurol. 2004; 474:304–324. [PubMed: 15164429]
47. Robinson GA. Immediate early gene expression in axotomized and regenerating retinal ganglion cells of the adult rat. Brain Res Mol Brain Res. 1994; 24:43–54. [PubMed: 7968376]

48. Tomita K, Ishibashi M, Nakahara K, et al. Mammalian hairy and Enhancer of split homolog 1 regulates differentiation of retinal neurons and is essential for eye morphogenesis. Neuron. 1996; 16:723–734. [PubMed: 8607991]

49. Chiodini F, Matter-Sadzinski L, Rodrigues T, et al. A positive feedback loop between ATOH7 and a Notch effector regulates cell-cycle progression and neurogenesis in the retina. Cell Rep. 2013; 3:796–807. [PubMed: 23434507]

50. Das AV, James J, Bhattacharya S, et al. SWI/SNF chromatin remodeling ATPase Brm regulates the differentiation of early retinal stem cells/progenitors by influencing Brn3b expression and Notch signaling. J Biol Chem. 2007; 282:35187–35201. [PubMed: 17855369]

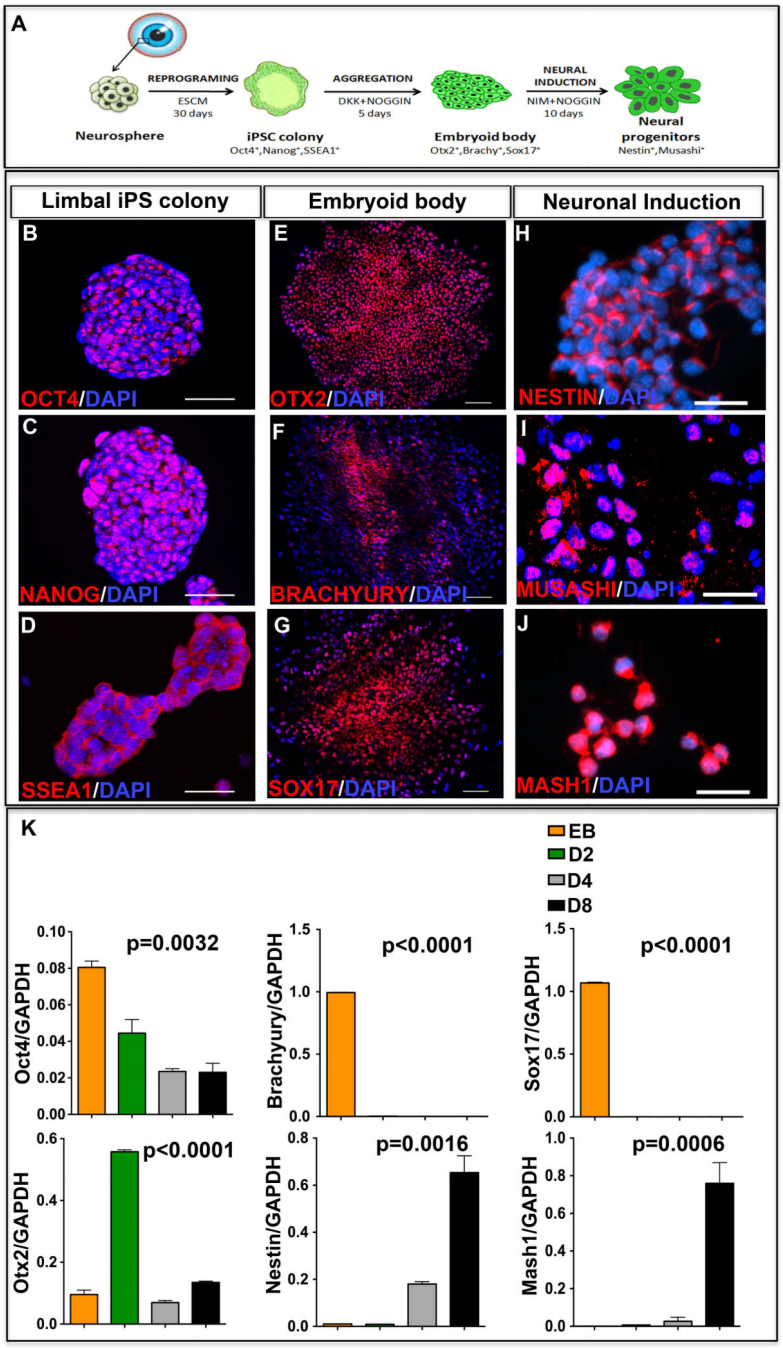

Figure 1. Reprogramming and neural induction of iPS cells

A schematic representation of non-cell autonomous reprogramming of cells from the limbus of the eye and neural induction of the resulting iPS cells is provided (A). The emerging iPS colonies expressed markers of pluripotency, Oct4 (B), Nanog (C) and SSEA1 (D). EBs generated by the hanging drop culture method expressed tri-lineage differentiation markers: Otx2 (ectoderm) (E), Brachyury (mesoderm) (F) and Sox −17 (ectoderm) (G). EBs cultured in the presence of neural induction medium (NIM) and Noggin, expressed immunoreactivities corresponding to Nestin (H), Musashi (I), and Mash1 (J). Q-PCR

analysis revealed a temporal decrease in the expression of *Oct4, Brachyury and Sox 17*, with increase in the expression of *Otx2, Nestin* and *Mash1* (K). *Otx2* expression decreased after day 2, presumably after initiating the neural induction. Scale bar: Panels B-D, H-J 50μm; Panels E-G 100μm.

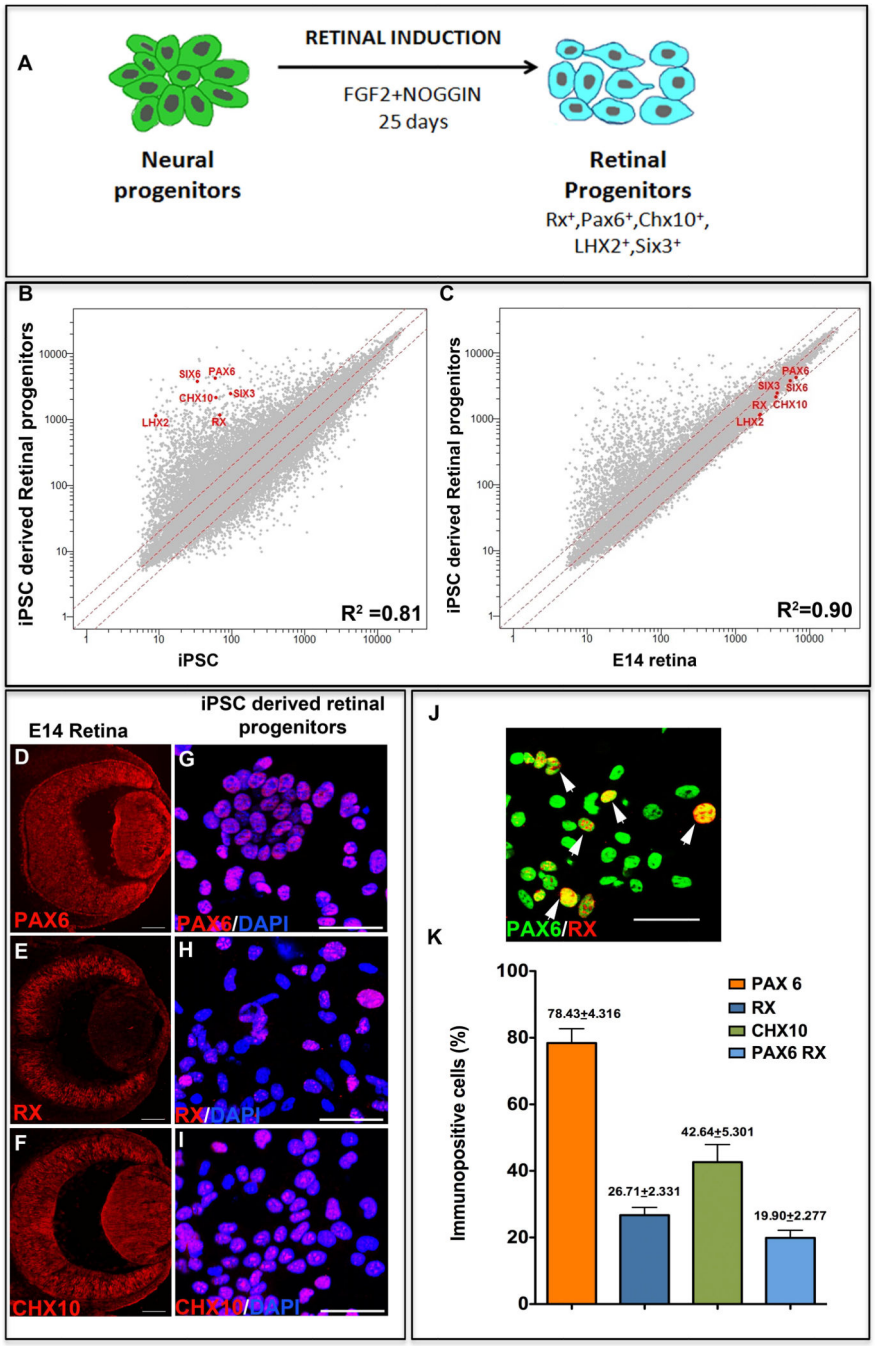

Figure 2. Generation of retinal progenitors from iPS cells

A schematic representation of the generation of retinal progenitors from iPS cell-derived neural progenitors is provided (A). Microarray analysis of un-induced and induced iPS cell-derived retinal progenitors at the end of retinal induction revealed global gene expression patterns with correlation coefficient R^2=0.81, displaying greater than two-fold increase in the gene expression levels of eye field genes (*Pax6, Rx, Six3, Chx10, Lhx2 and Six6*) in the latter (B). Microarray analysis of induced iPS cell-derived neural progenitors and E14 retina revealed a positive correlation in the global gene expression patterns (R^2=0.9) with

comparable (less than two-fold difference) gene expression levels of the eye field genes (C). Immunocytochemical analysis of the iPS cell-derived neural progenitors, at the end of retinal induction, revealed a subset of cells expressing immunoreactivities corresponding to Pax6 (G, K), Rx (H, K) and Chx10 (I, K) similar to retinal progenitors in the E14 retina (D–F). A subset of cells co-expressed immunoreactivities corresponding to both Pax6 and Rx (white arrowheads) (J, K). Scale bar: Panels D–F 200μm; Panels G-J 50μm.

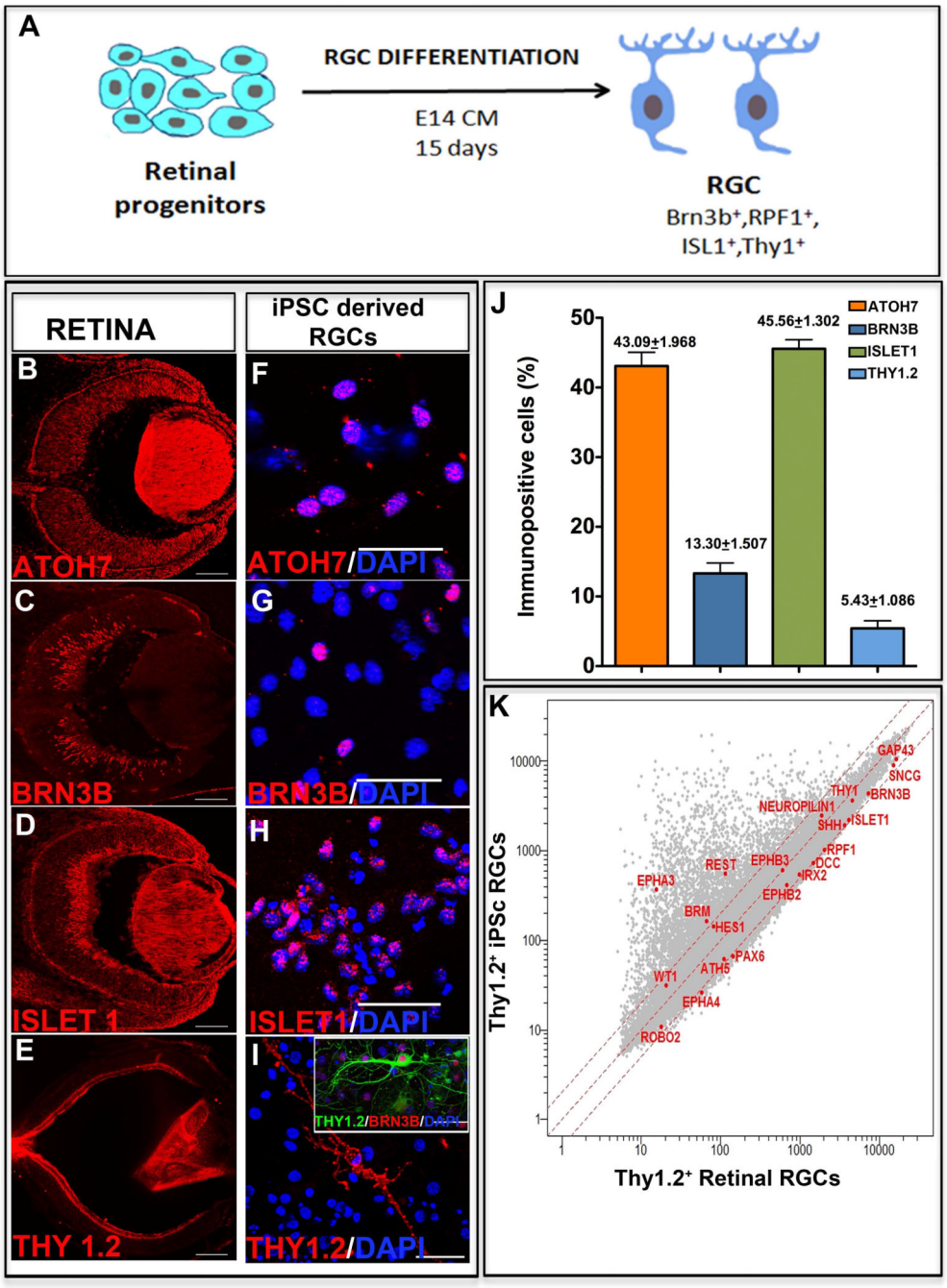

Figure 3. Generation of RGCs from iPS cell-derived retinal progenitors

A schematic of RGC differentiation protocol is provided (A). Immunocytochemical analysis of the iPS cell-derived retinal progenitors at the end of RGC differentiation revealed a subset of cells expressing immunoreactivities corresponding to Atoh7 (F, J), Brn3b (G, J), and islet1 (H,J) similar to RGCs in the E14 retina (B–D). These cells also expressed matured RGC markers Thy1.2 (I,J) as in PN1 retina (E). The Thy1.2^{+} cells co-expressed Brn3b immunoreactivities (I, inset). Microarray analysis of Thy1.2^{+} iPS cell-derived RGCs and Thy 1.2^{+} native retinal RGCs showed global gene expression pattern with correlation

coefficient R^2=0.82 with comparable (less than two-fold difference) gene expression levels of most RGC regulators and markers (K). Scale bar: Panels B–E 200μm; Panels F–I 50μm.

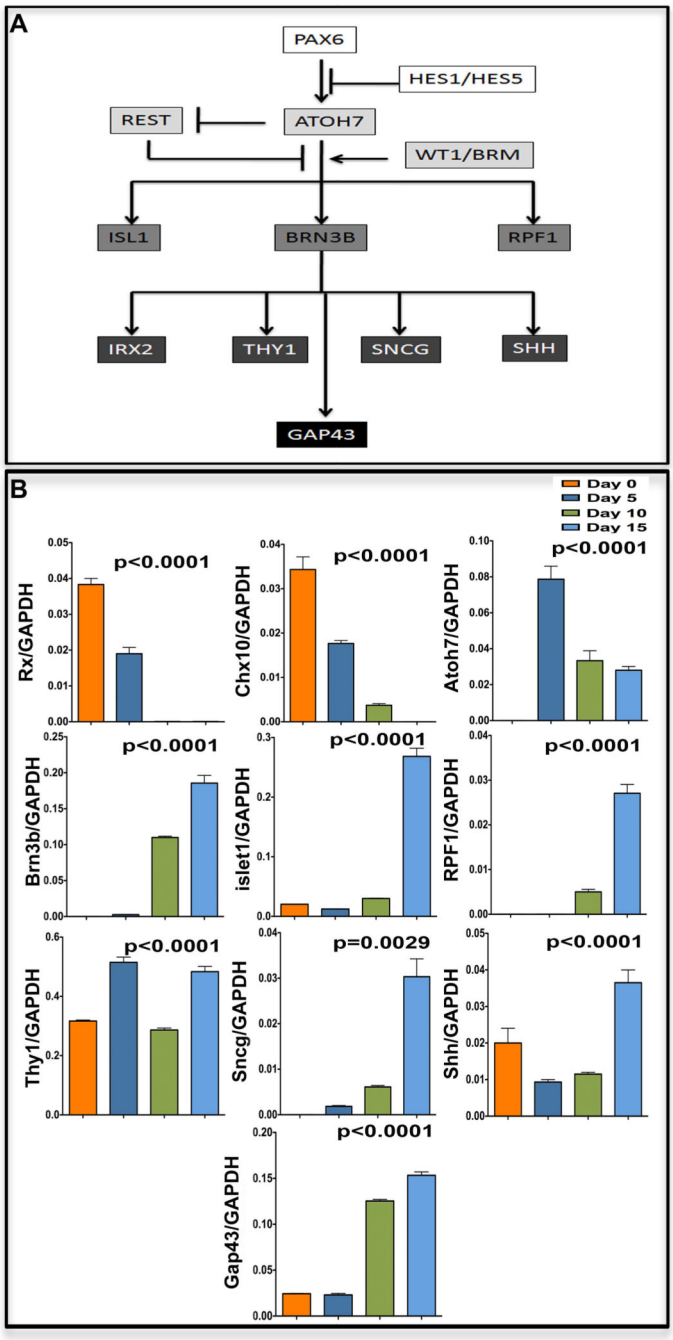

Figure 4. Temporal expression patterns of RGC regulatory genes during RGC differentiation

A schematic representation of gene regulatory hierarchy for RGC specification and differentiation is provided (A). Q-PCR analysis revealed a temporal decrease in the expression of Rx and Chx10 as RGC differentiation proceeded, with concordant temporal increase in the expression of regulators and mature markers (*Atoh7*, *Brn3b*, *Isl1*, *RPF1*, *Sncg*, *Shh*, *Thy1*, and *GAP43*) of RGCs (B).

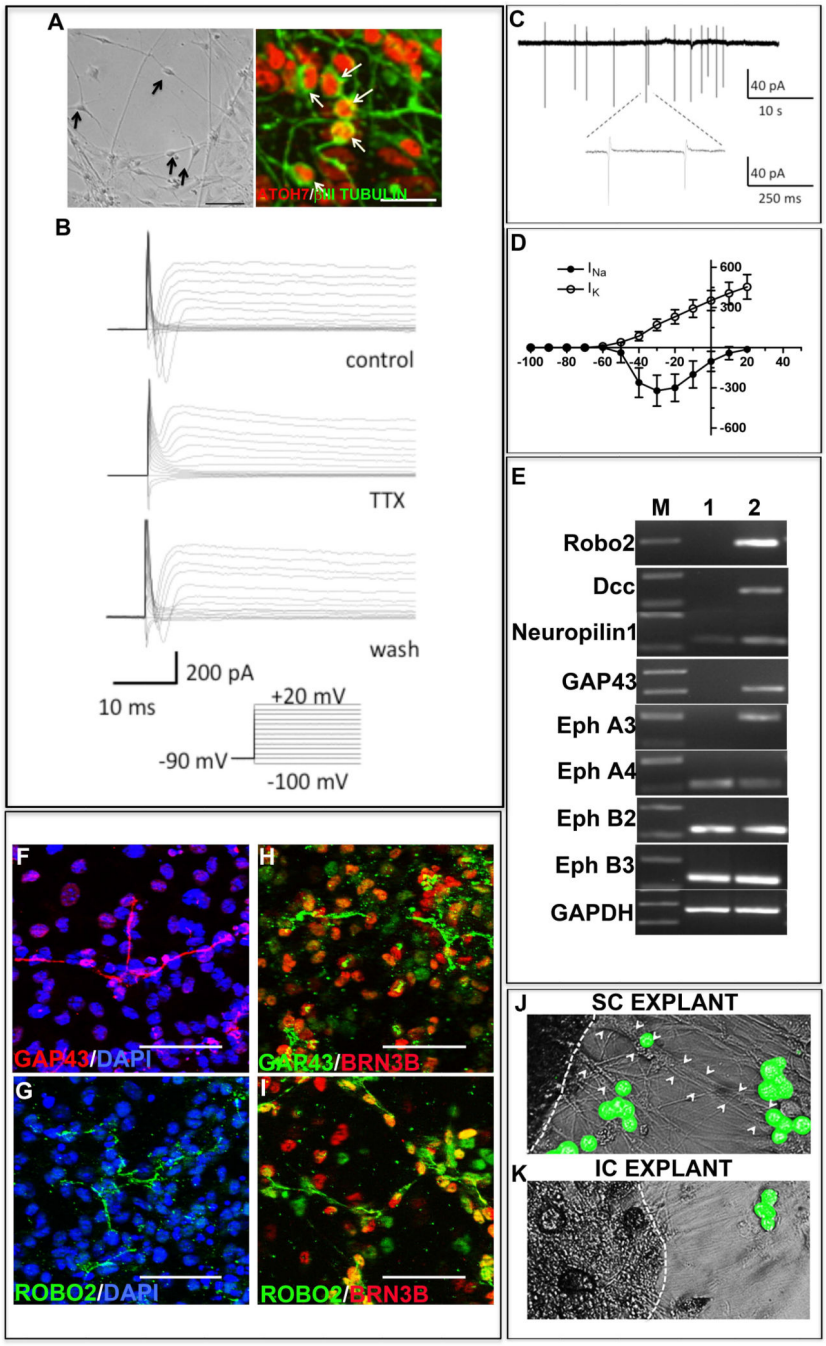

Figure 5. Functional characteristics and target specificity of iPS cell-derived RGCs

To examine the functional characteristics of iPS cell-derived RGCs, whole cell patch recordings of cells with neuronal morphologies (A) co-expressing Atoh7 and β III Tubulin (magnified to appreciate details of the image represented in phase) were carried out which revealed the presence of fast inward and delayed outward currents in 85.71% of cells (n=14), the former being TTX sensitive (**B**). Cells examined in loose-patch conditions, elicited spiking activities with frequencies ranging from 0.08 to 0.3 Hz in 71.43% of cells analyzed (n=15) (**C**). The fast inward and outward currents showed I-V relationship typical

of voltage–gated sodium and delayed potassium currents, respectively (**D**). To examine the potential of iPS cell-derived RGCs to form connections with bona fide targets we examined the expression of axon guidance molecules. RT-PCR revealed that in comparison to retinal progenitors controls (lane 1) RGCs (Lane 2) expressed higher levels of Robo2, DCC, NRP1, GAP43, and EPHs transcripts (**E**). These RGCs expressed immunoreactivities corresponding to GAP43 (**F**) and Robo2 (**G**) co-localized with that of Brn3b (**H, I**). CFDA-tagged iPS cell-derived RGCs elaborated processes to cells of superior colliculus (SC) (**J**) and not to inferior colliculus (IC) (**K**) cell aggregates, demonstrating target specificity. Scale bar: 200 μm (A, phase); 20μm (A, Fluorescence image) 50μm (F–I).

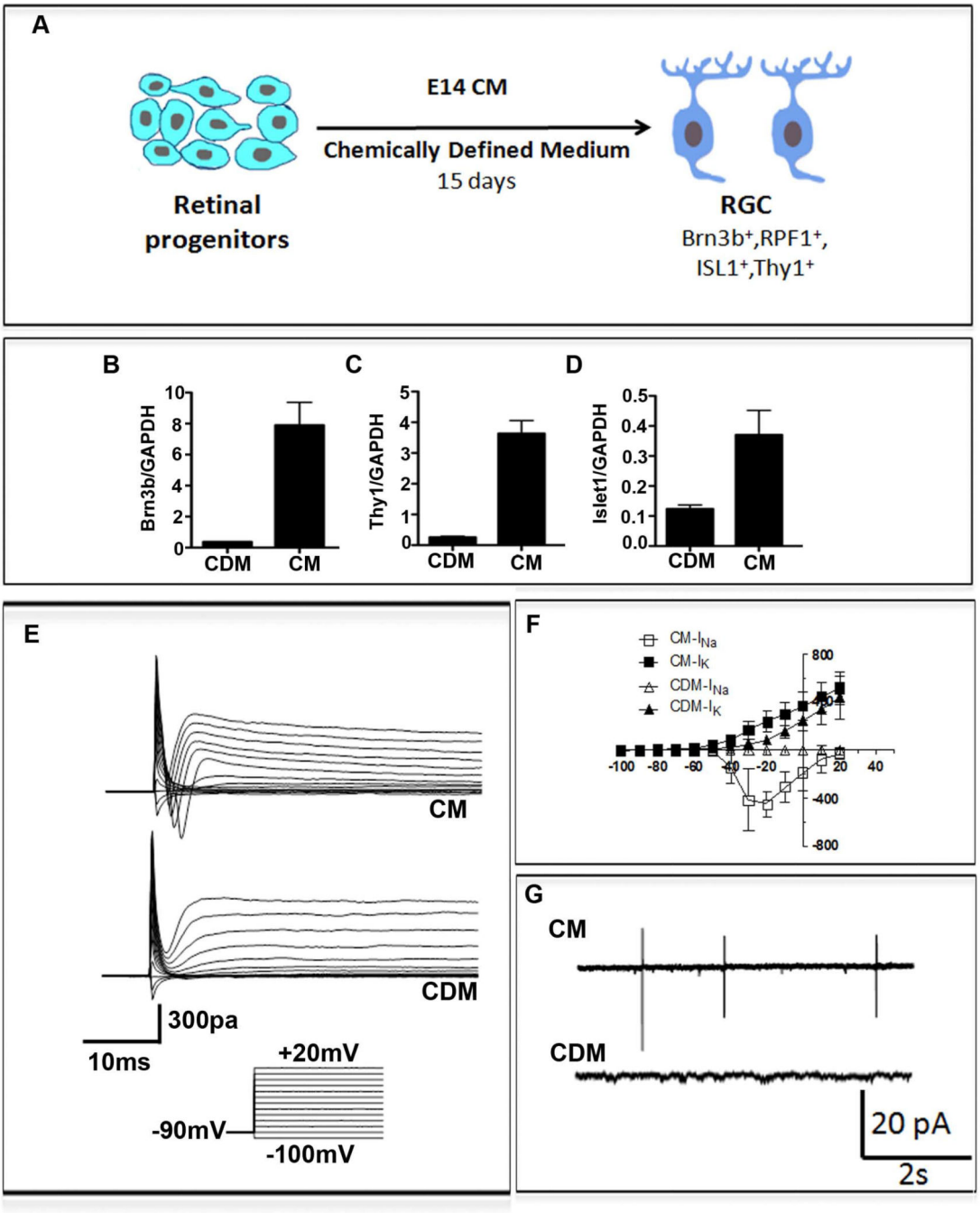

Figure 6. A Comparison of E14CM and CDM-mediated directed differentiation of iPS cell-derived retinal progenitors

A schematic of RGC differentiation protocol under E14CM/CDM is provided (A). Q-PCR analysis revealed that cells in CDM expressed significantly lower levels of transcripts corresponding to *Brn3b*, Thy1, and *Islet1*, compared to those cultured in E14CM (B–D). To examine the functional characteristics of iPS cell-derived RGCs in CDM and E14CM, whole cell patch recordings of cells were carried out, which revealed the presence of fast inward and delayed outward currents in cells cultured in E14CM (n=4) (E). In contrast, cells

cultured in CDM displayed only sustained outward currents (n=10). The fast inward and outward currents in cells cultured in E14CM showed I-V relationship typical of voltage–gated sodium and delayed potassium currents, respectively (**F**). Cells in CDM showed only delayed but sustained outward currents above −60mV (**F**). Cells examined in loose-patch conditions, elicited spiking activities only in E14CM and not in CDM (n=4) (**G**).

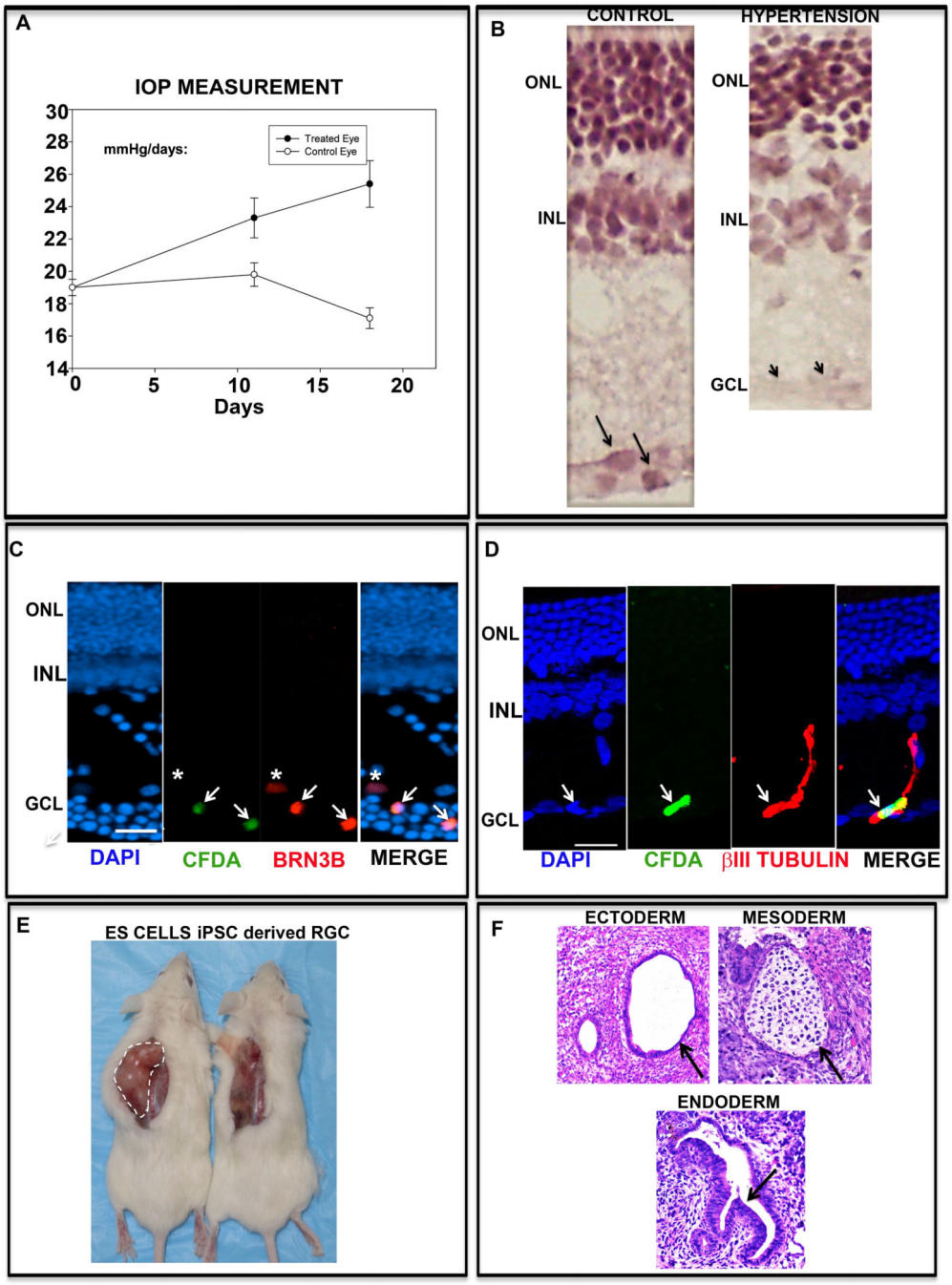

Figure 7. Transplantation of iPS cell-derived RGCs in ocular hypertensive rats and NOD-SCID mice

IOP measurement of rats subjected to ocular hypertension revealed slow but progressive increase in the intra-ocular pressure (IOP) in the treated eye and not in the control eye (A). Hematoxylin and eosin staining of a section of ocular hypertensive retina revealed a thinner inner plexiform layer and a select area of ganglion cell layer lacking cells, compared to controls, demonstrating degenerative changes (B). Immunohistochemical analyses of iPS cell-derived retinal progenitors, pre-exposed to RGC differentiation, labeled with CFDA, and transplanted intravitreally into ocular hypertensive rats revealed lamina specific

integration of CFDA positive cells (arrows), expressing Brn3b (C) and β-III tubulin (D) immunoreactivities. A $CFDA^{-}$ $Brn3b^{+}$ (native RGC) cell is identified by an asterisk. Subcutaneous injection of iPS cell-derived RGCs did not produce teratoma in the NOD-SCID mice unlike the ES cells (positive control) (E). The teratoma generated by the ES cells revealed the presence of all the three embryonic lineages ectoderm (duct); mesoderm (cartilage) and endoderm (glandular columnar epithelium) (F).